

A unifying approach to left handed material design

Jiangfeng Zhou,¹ Eleftherios N. Economou,² Thomas Koschny,^{3,4} and Costas M. Soukoulis^{3,4}

¹*Department of Electrical and Computer Engineering and Microelectronics
Research Center, Iowa State University, Ames, Iowa 50011*

²*Institute of Electronic Structure and Laser - FORTH,
and Department of Physics, University of Crete, Greece*

³*Ames Laboratory and Department of Physics and Astronomy, Iowa State University, Ames, Iowa 50011*

⁴*Institute of Electronic Structure and Laser - FORTH,
and Department of Materials Science and Technology, University of Crete, Greece*

In this letter we show that equivalent circuits offer a qualitative and even quantitative simple explanation for the behavior of various types of left-handed (or negative index) meta-materials. This allows us to optimize design features and parameters, while avoiding trial and error simulations or fabrications. In particular we apply this unifying circuit approach in accounting for the features and in optimizing the structure employing parallel metallic bars on the two sides of a dielectric film. Pacs: 42.70.Qs, 41.20.Jb, 42.25.Bs, 73.20.Mf

Left-handed materials exhibit a negative permeability, μ , and permittivity, ϵ , over a common frequency range [1]. Negative permeability is the result of a strong resonance response to an external magnetic field; negative permittivity can appear either by a plasmonic or a resonance response (or both) to an external electric field. Negative μ and negative ϵ lead to negative index of refraction, n , and to a left-handed triad of $\vec{k}, \vec{E}, \vec{H}$; hence, the names negative index materials (NIMs) or Left-handed Materials (LHMs). Pendry[2, 3] suggested a double metallic split-ring resonator (SRR) design for negative μ and a parallel metallic wire periodic structure for an adjustable plasmonic response. Several variation of the initial design have been studied; among them a single ring resonator with several cuts has been proved capable of reaching negative μ at higher frequency [4]; in Fig. 1(a) a two cut single ring is shown schematically. This, by a continuous transformation, can be reduced to a pair of carefully aligned metal bars separated by a dielectric spacer of thickness t_s [5, 6]; in Figs 1(b) and 1(c) the view in the (\vec{E}, \vec{k}) and (\vec{E}, \vec{H}) planes of this structure is shown together with the directions of $\vec{k}, \vec{E}, \vec{H}$ of the incoming EM field.

The design shown in Figs 1(b,c), besides its simplicity, has distinct advantages over conventional SRRs. The incident electromagnetic wave is normal to the structure as shown in Fig. 1(b), which enable us to build NIMs by only one layer of sample and achieve relatively strong response. Conventional SRRs, although they exhibit magnetic resonance which may produce negative μ , they fail to give negative ϵ at the same frequency range and, hence, they are incapable by themselves to produce NIMs. An extra continuous wire is needed to obtain negative ϵ via plasmonic response [2, 7]. In contrast, the pair of parallel metallic plates is expected to exhibit not only a magnetic resonance [Fig. 2(c), antisymmetric mode], but to show an electric resonance as well [symmetric mode] properly located in frequency by adjusting the length, l , of the pair.

The simulations were done with the CST Microwave

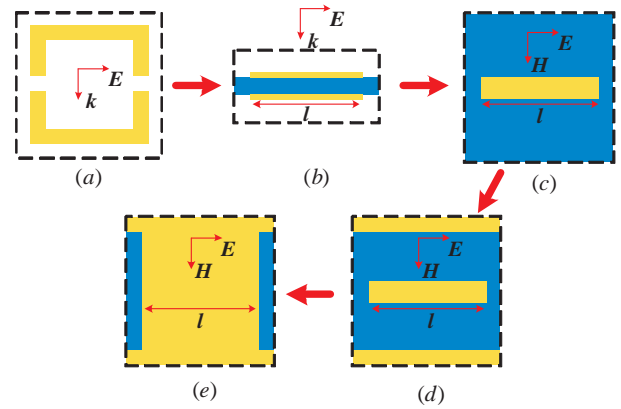


FIG. 1: (Color online) The two cut single metallic SRR (a) can be transformed to a pair of parallel metallic bars separated by a dielectric (b, view in (\vec{E}, \vec{k}) plane; c, view in (\vec{E}, \vec{H}) plane). By adding continuous wires, design d (view in (\vec{E}, \vec{H}) plane) results, which can be modified to a fully connected one on both sides of the thin dielectric board (e). The dashed square defines the unit cells with dimension a_x (parallel to \vec{H}), a_y (parallel to \vec{E}) and a_z (parallel to \vec{k}).

Studio (Computer Simulation Technology GmbH, Darmstadt, Germany) using the lossy metal model for copper with a conductivity $\sigma = 5.8 \times 10^7$ for a single unit cell with periodic boundary in the (E, H) plane, field distribution and scattering amplitudes have been calculated. The ϵ, μ in Fig. 6 have been obtained by a retrieval procedure [8]. At the magnetic resonance the two plates sustain anti-parallel currents producing a magnetic field \vec{B} confined mainly in the space between the plates and directed opposite to that shown in Fig. 1(c); the electric field, because of the opposite charges accumulated at the ends of the two plates, is expected to be confined within the space between the plates and near the end points. Indeed, detailed simulations, shown in Fig. 2(c), confirm this picture.

At the electric resonance the currents at the two bars

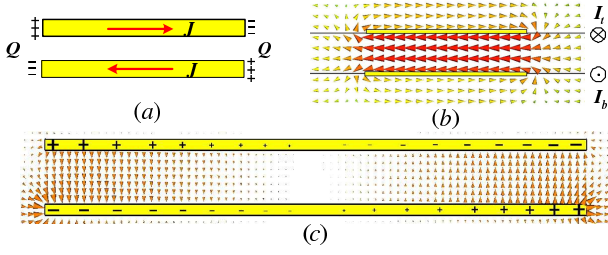


FIG. 2: (Color online) At the magnetic resonance the currents (a, in (\vec{E}, \vec{k}) plane, view in \vec{H} direction), the magnetic field (b, in (\vec{H}, \vec{k}) plane) and the electric field (c, in (\vec{E}, \vec{k}) plane) are shown. Sizes of the cones show the intensity of magnetic field \vec{H} (b) and electric field \vec{E} (c) in logarithm scale.

are parallel (symmetric mode); the magnetic field lines go around both bars, while the electric field is mostly confined in the space between the nearest neighbor edges of the two pairs of bars belonging to consecutive unit cells.

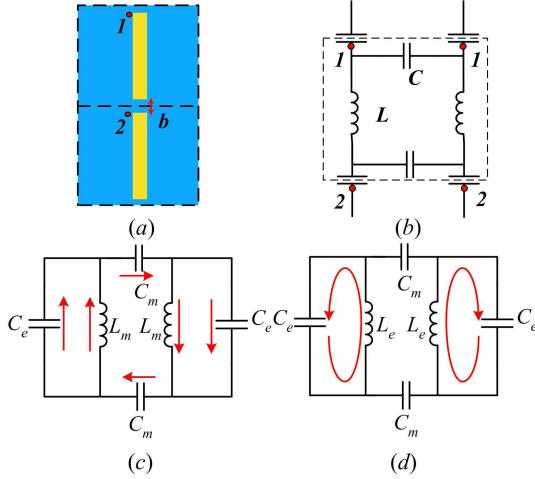


FIG. 3: (Color online) Current distribution of the two parallel metallic bar design (a) (side view, the parallel plates are behind one another) can be accounted for by the equivalent circuit (b), which, since points 1 and 2 are equivalent because of the periodicity, reduces to circuit (c) and (d) for the magnetic (c) and electric (d) resonance respectively.

The field and current configurations for both the antisymmetric and the symmetric mode can be accounted for by equivalent R, C, L circuits as shown in Fig. 3 (in which for simplicity the resistor elements have been omitted). Near the magnetic resonance frequency where the current configuration is as in Fig. 3(c), the magnetic field is between the two plates and it is, to a good approximation, uniform (Fig. 2(b)). Hence the total inductance L , as calculated by the magnetic field energy, is

$$L = 2L_m \simeq \mu \frac{t_s}{w} l, \quad (1)$$

where l is the length of the wire, t_s is the thickness of the dielectric spacer and w is the width of the wire.

Notice that at telecommunication or optical frequencies, where the linear dimension are in the tens or hundreds of nm, the kinetic energy of the drifting electrons makes a contribution comparable or larger than the magnetic energy. Hence, another additional inductance must be added to the right hand side of Eq.1 [4].

Each of the capacitance C_m must be given by a formula of the type

$$C_m = \frac{\epsilon w l'}{t_s}, \quad (2)$$

where by inspection of Fig. 2(c), $l' = c_1 l$ with the numerical factor c_1 in the range $0.2 \leq c_1 \leq 0.3$. The capacitance C_e can be approximated by that of two parallel wires of radius t_m and length w at a distance b apart

$$C_e = \frac{\pi \epsilon w}{\ln(b/t_m)}, \quad (3)$$

where t_m is the thickness of each metallic bar and b is the separation of neighboring pairs Fig. 3(a,b) ($b = a_y - l$). The magnetic resonance frequency, ω_m , is obtained by equating the impedance Z (of L_m and C_e in parallel) with minus the impedance $-i/C_m \omega$ of the capacitance C_m .

Since $Z = iL_m \omega / (1 - L_m C_e \omega^2)$ we obtain

$$\omega_m = \frac{1}{\sqrt{L_m(C_m + C_e)}} \simeq \frac{1}{\sqrt{L_m C_m}}. \quad (4)$$

The last relation follows because, for the values we have used ($l = 7\text{mm}$, $w = 1\text{mm}$, $t_s = 0.254\text{mm}$, $t_m = 10\mu\text{m}$ and $b = 0.3\text{mm}$), $C_e \simeq 0.1C_m$. Combining the Eq.1 and Eq.2 we find that

$$f_m = \frac{\omega_m}{2\pi} = \frac{1}{2\pi l \sqrt{\epsilon \mu} \sqrt{c_1/2}} = \frac{1}{2\pi \sqrt{c_1 \epsilon_r/2}} \frac{c}{l} \quad (5)$$

where $\epsilon_r = 2.53$ is the reduced dielectric constant of the dielectric, $\epsilon_r = \epsilon/\epsilon_0$. In Fig.4 we compare our result of Eq.5, which shows that f_m is a linear function of only $1/l$, with detailed simulations results. Fig. 4 shows the dependence of the magnetic resonance frequency as obtained from the retrieved resonant effective μ on the inverse length of the parallel metallic bars (Fig. 1b), for different widths w (separation between parallel bars $t_s = 0.254\text{mm}$ fixed) and two different separations t_s (width of bars $w = 1\text{mm}$ fixed). Complete quantitative agreement is obtained if $c_1 = 0.22$. Notice the independence of the simulation results on the width w and the dielectric thickness t_s . It is worthwhile to point out that the result $f_m \sim 1/l$ is robust over a wide range of parameters even if Eqs. 1 and 2 are not valid. To see this point, consider the extreme case of a pair of thin wires (as opposed to a pair of bars) of length l , cross-section radius r , at a distance d apart such that $r \ll d \ll l$. For such a system $L = (\mu/4\pi)[1 + 4 \ln(d/r)] \simeq (\mu l/\pi) \ln(d/r)$ and $C \simeq \pi l / \ln(d/r)$. Thus again $f_m \sim 1/\sqrt{\epsilon \mu} l$.

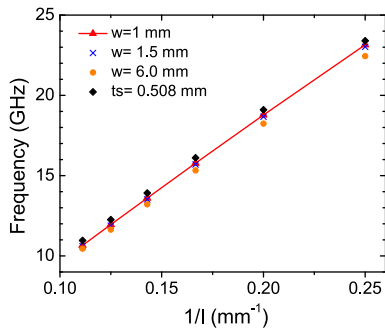


FIG. 4: (Color online) Linear dependence of the magnetic resonance frequency, f_m , as obtained by simulation, on the inverse length l ; this result as well as its independence on w and t_s is in agreement with the simple formula (5). ($t_s = 0.254\text{mm}$ for triangular, cross, circle; $w = 1\text{mm}$ for diamond; and for all cases, $b = 0.5 \sim 5.5\text{mm}$, $a_x = 20\text{mm}$).

For frequencies near the electric resonance, because of mirror symmetry in Fig. 3(d), there is no current passing through the capacitances C_m . As a result the electric resonance frequency f_e is given by $f_e = 1/(2\pi\sqrt{C_e L_e})$, where L_e is expected to be of the form $(\mu/\pi)g(w/l)$ where $g(x)$ is a function which for $x \rightarrow 0$ behaves as $-\ln(x)$.

We point out that f_e is a rather sensitive function of the small distance b , because C_e depends on b , while L_e is practically independent on b . Indeed the ratios $f_e(2b)/f_e(b)$ and $f_e(3b)/f_e(b)$ for $b = 0.1\text{mm}$ according to the equation of C_e and equation of f_e are respectively 1.14 and 1.215 in good agreement with the simulation results in Fig. 5 (1.13 and 1.21 respectively); the dependence of both f_m and f_e on $a_y/l = 1 + b/l$ is shown in Fig. 5.

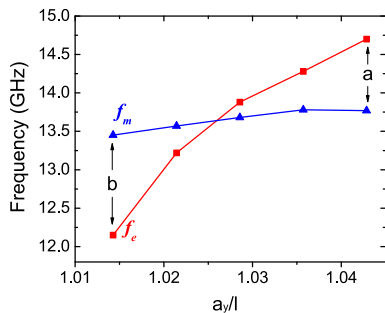


FIG. 5: (Color online) Magnetic resonant frequency f_m cross over with electrical resonant frequency f_e as $a_y/l = 1 + b/l$ varies between 7.1mm and 7.3mm ; $a_x = 20\text{mm}$.

Fig. 5 in combination with Fig. 6 suggest the optimum design parameters for making the two bar scheme to produce negative index n : One has to avoid the crossing region where essentially to a considerably degree the two resonances cancel each other. Since the electric reso-

nance is much stronger and, hence, much wider we have to bring the magnetic resonance within the negative region of ϵ , i.e. we must have f_e lower than f_m as in Fig. 6(b), rather than the other way around, i.e. we must have

$$\left(\frac{f_e}{f_m}\right)^2 = \frac{L_m}{L_e} \left(1 + \frac{C_m}{C_e}\right) < 1 \quad (6)$$

This can be achieved by increasing C_e either by decreasing b or by increasing at the ends of each bar the width w choosing a double T shape for each bar [9].

Still another possibility to make the negative ϵ region wider (and more negative) is to add continuous metallic wires as in Fig. 1(d) which produce a plasmonic response [5]. By adjusting the width of these wires their effective plasma frequency f_p can be made larger than the frequency, f_1 , at which the continuous curve in Fig. 6(b) crosses the axis ($f_1 \simeq 16\text{GHz}$).

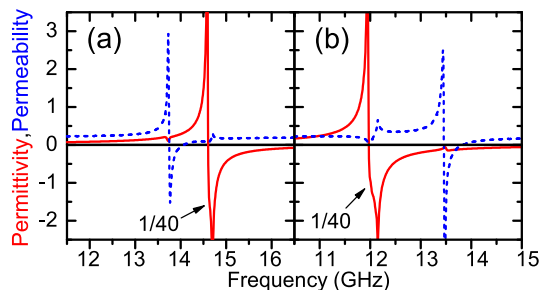


FIG. 6: (Color online) Retrieved ϵ_{eff} (solid lines) and μ_{eff} (dotted lines) for two cut wires. (a) and (b) correspond to points a ($a_y = 7.3\text{mm}$, $a_x = 20\text{mm}$) and b ($a_y = 7.1\text{mm}$, $a_x = 20\text{mm}$) in Fig. 5. Notice that both the response are Lorentz like.

Finally the width of the bars, w , can increase until the bars join the "infinite" wires producing thus a continuous connected network which can be constructed by opening periodically placed rectangular holes on uniform metallic films covering both sides of a dielectric sheet [10, 11, 12].

In this letter we have shown that L, C equivalent circuits can account for the EM properties of various negative index artificial meta-materials (NIMs), even at a quantitative level; furthermore, this simple unifying circuit approach offers a clear guidance in adjusting the design and optimizing the parameters for existing and possibly, future NIMs.

We gratefully acknowledge the support of Ames Laboratory (operated by Iowa State University under Contract No. W-7405-Eng-82), the AFOSR under MURI grant (FA9550-06-1-0337), EU Network of Excellence projects METAMORPHOSE and PHOREMOST, and Defence Advanced Research Projects Agency (DARPA) contract HR0011-05-C-0068).

-
- [1] V. Veselago, *Sov.Phys. Usp.* **10**, 509 (1968).
- [2] J. Pendry, A. Holden, W. Stewart, and I. Youngs, *Physical Review Letters* **76**, 4773 (1996).
- [3] J. Pendry, A. Holden, D. Robbins, and W. Stewart, *IEEE Trans. Microwave Theory Tech.* **47**, 2075 (1999).
- [4] J. Zhou, T. Koschny, M. Kafesaki, E. N. Economou, J. B. Pendry, and C. M. Soukoulis, *Physical Review Letters* **95**, 223902 (pages 4) (2005), URL <http://link.aps.org/abstract/PRL/v95/e223902>.
- [5] J. Zhou, L. Zhang, G. Tuttle, T. Koschny, and C. M. Soukoulis, *Physical Review B (Condensed Matter and Materials Physics)* **73**, 041101 (pages 4) (2006), URL <http://link.aps.org/abstract/PRB/v73/e041101>.
- [6] V. M. Shalaev, W. S. Cai, U. K. Chettiar, H. K. Yuan, A. K. Sarychev, V. P. Drachev, and A. V. Kildishev, *Optics Letters* **30**, 3356 (2005).
- [7] D. Smith, W. Padilla, D. Vier, S. Nemat-Nasser, and S. Schultz, *Physical Review Letters* **84**, 4184 (2000).
- [8] D. R. Smith, S. Schultz, P. Markos, and C. M. Soukoulis, *Physical Review B (Condensed Matter and Materials Physics)* **65**, 195104 (pages 5) (2002), URL <http://link.aps.org/abstract/PRB/v65/e195104>.
- [9] J. Zhou, T. Koschny, L. Zhang, G. Tuttle, and C. M. Soukoulis, *Applied Physics Letters* **88**, 221103 (pages 3) (2006), URL <http://link.aip.org/link/?APL/88/221103/1>.
- [10] G. Dolling, C. Enkrich, M. Wegener, C. M. Soukoulis, and S. Linden, *Science* **312**, 892 (2006).
- [11] S. Zhang, W. Fan, B. K. Minhas, A. Frauenglass, K. J. Malloy, and S. R. J. Brueck, *Physical Review Letters* **94**, 037402 (pages 4) (2005), URL <http://link.aps.org/abstract/PRL/v94/e037402>.
- [12] S. Zhang, W. Fan, N. C. Panoiu, K. J. Malloy, R. M. Osgood, and S. R. J. Brueck, *Physical Review Letters* **95**, 137404 (pages 4) (2005), URL <http://link.aps.org/abstract/PRL/v95/e137404>.